FTD-ID(RS)T-0306-90

FOREIGN TECHNOLOGY DIVISION

THEORY AND SIMULENT DESIGN OF A TYPE OF AUTO-SELF-PROTECTING OPTICAL SWITCHES

by

Li Binhong, Peng Songcun

HUMAN TRANSLATION

FTD-ID(RS)T-0306-90 11 June 1990

MICROFICHE NR: FTD-90-C-000596

THEORY AND SIMULENT DESIGN OF A TYPE OF AUTO-SELF-PROTECTING OPTICAL SWITCHES

By: Li Binhong, Peng Songcun

English pages: 17

Source: Shanghai Jiaotong Daxue Xuebao, Nr. 6, 1984, pp. 11-23

Country of origin: China
Translated by: Leo Kanner Associates
F33657-88-D-2188
Requester: FTD/TTTD/Scanlon

PREPARED BY:

TRANSLATION DIVISION
FOREIGN TECHNOLOGY DIVISION
WPAFB, OHIO.

GRAPHICS DISCLAIMER

All figures, graphics, tables, equations, etc. merged into this translation were extracted from the best quality copy available.

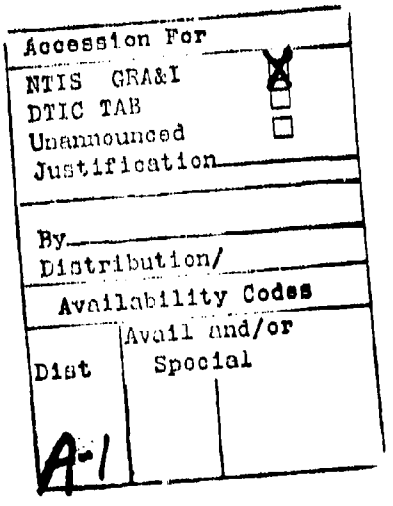

THEORY AND SIMULENT DESIGN OF A TYPE OF AUTO-SELF-PROTECTING OPTICAL SWITCHES

Li Binhong, Peng Songcun (S.T. Peng, professor at New York Institute of Science and Engineering, consulting professor at Jiaotong University)

Received 17 September 1983, revised 26 June 1984.

ABSTRACT

Based upon a study of the transmitting and scattering characteristics of multilayer dielectric optical wave guides, a practical computer program is set up for designing a type of auto-self-protecting optical switch with a computer model by using the nonlinear property of dielectric layers and the plasma behavior of metal substrates. This technique can be used to protect the human eye and sensitive detectors from damage caused by strong laser beams.

1. FOREWORD

As the use of lasers in the military and in the civilian economy increases with each passing day, it is often necessary for the human eye or sensitive instruments to observe weak lasers, such as the return waves of laser radar and laser communications signals; but it is also necessary to provide protection against damage to the eye from the strong lasers of enemy laser weapons. For this reason, it is necessary to have a kind of automatic optical self-protecting switch; its principle is as shown in Fig. 1. For weak lasers, at the angle of observation θ_0, it is possible to observe signals; in the case of strong lasers, θ_0 is the angle of absorption, protecting the eye or the instrument. The authors present the theory behind a kind of automatic optical self-protecting switch, and use a computer model to calculate several possible structural types that can serve as the basis for practical devices.

This kind of switch is a structure with multiple layers. When a weak optical signal (multiple layer structure's reflection wave) is observed from a given angle, the wave has very little attenuation, and provides normal observation. When, however, a strong beam is monitored, this observation angle immediately and automatically becomes the angle of absorption, with a great attenuation. When the strong beam ceases, the angle again immediately

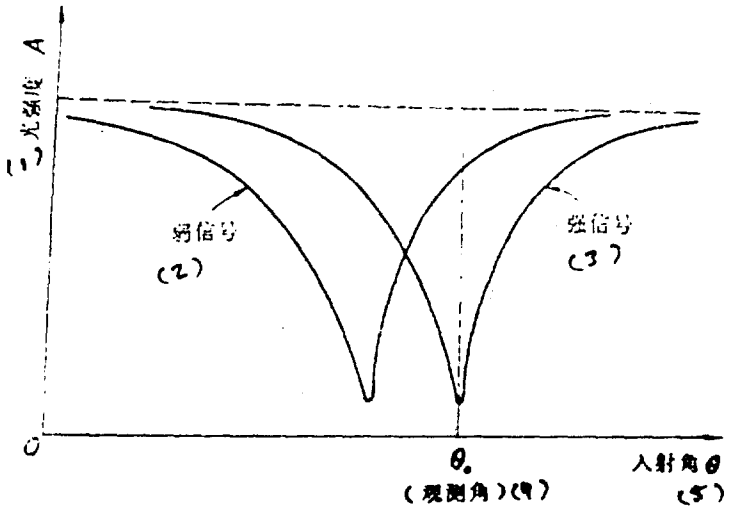

Fig. 1. Principle of a kind of automatic optical self-protecting switch. Key: (1) Optical intensity; (2) Weak signal; (3) Strong signal; (4) Angle of observation; (5) Angle of incidence.

reverts to the normal observation angle for weak signals, and continues to function. The absorption mechanism of the multilayer structure with respect to the incident light (plane wave) is to couple the incident wave into the multilayer structure to become a guide wave, causing it to be absorbed during the transmission process by the damaged layer. The problem of how to make a TE wave and a TM wave reach a high rate of absorption has been solved by the authors in another paper [1]. The authors have also found a design method which achieves 100% absorption (forthcoming paper). To make a self-protecting optical switch, it is necessary to give the two kinds of polarized waves (TE waves and TM waves) an identical absorption rate and angle of absorption; furthermore the angle of absorption of the two kinds of waves can perform synchronous shifting according to the incident power. This is the problem that this paper intends to solve. This kind of automatic synchronized function in instruments is achieved by means of two physical phenomena: The non-linear nature of a given dielectric layer and the plasma characteristics of the metallic substrate.

By the non-linear nature of a dielectric, we mean that its dielectric constant ϵ is the function $\epsilon(E)$ of the electromagnetic field's strength (E, in this case). Speaking theoretically, because of changes in a given layer's

ϵ , the transmission constant and the relative speed of the entire structure's guide wave will vary accordingly; the incident angle during coupling will change on this basis, and the angle of absorption will undergo a shift. The difficulty is in maintaining the synchronous shifting of the angle of absorption of the two polarized waves, because it is commonly said that the angle of absorption of TE and TM waves differ in accordance with the migration rate of ϵ (E). This difficulty is solved by means of using the absorption principle of the TM wave jumping pattern (from a common surface wave TM pattern to a plasma surface wave TM pattern).

It is known from the plasma electromagnetic field eigenvalue theory that metals, under optical frequencies, show the characteristics of plasmas, having a great real negative value dielectric constant ϵ', and carrying a relatively small virtual value ϵ''. For example, under an optical frequency, $\dot{\epsilon} = \epsilon' - j\epsilon'' \approx -16.0 - j0.8$ and so on. From guide wave theory, we can infer that at the dividing surface between plasma and dielectric there exists a special TM surface wave, called a plasma surface pattern (see section 2 below). It is this kind of peculiar surface wave that we use to solve the difficulties of the lack of synchronization between the angles of absorption of the two kinds of polarized waves as the field strength shifts. It is possible to discover a structure that under a weak field causes the common surface wave TE pattern and the common surface wave TM pattern to have an identical absorption angle and absorption rate; and that, with a strong field, causes the common surface wave TE pattern and the plasma surface wave TM pattern to have an identical angle of absorption (naturally, not the same one as the absorption angle under a weak field) and absorption rate. This achieves the synchronous jumping variation of the absorption curve (or reflection curve) of the two kinds of polarized light.

For the theoretical analysis in this paper, we use the network method to solve the eigenvalue problem for multiple layer structures, and find the reflection coefficient. This method is rigorous, and is suitable for making design calculations using computers.

2. THEORETICAL ANALYSIS

For the sake of widespread applicability, we do not for the time being delimit the structure's number of layers. Assume an n-layer dielectric, with corresponding dielectric constants of ϵ_1, ϵ_2, ..., ϵ_n, and thicknesses of t_1, t_2, ..., t_n. The base is a substrate with a dielectric constant of ϵ_s, and the top layer is a prismatic region with a dielectric constant of ϵ_p. The gap between it and the ϵ_1 layer is an empty interval with a dielectric constant of ϵ_a and a thickness of t_a. Further, assume a plane optical wave entering from the prismatic region with an incident angle of θ, and an incident wave and a reflection wave respectively of *a* and *b*, as shown in Fig. 2.

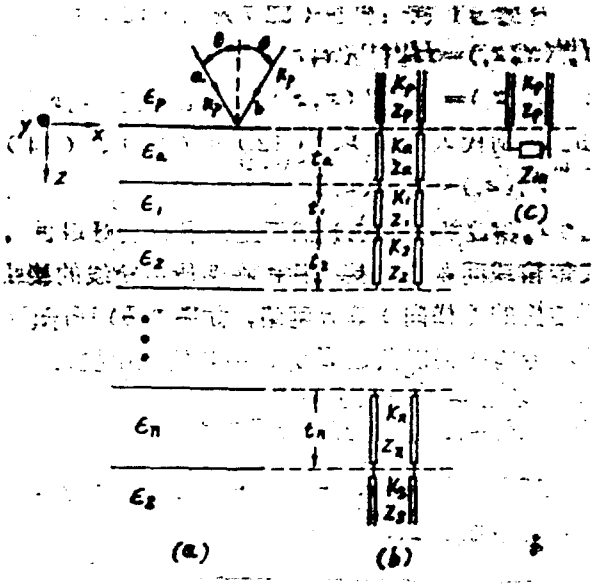

Fig. 2. Multilayer dielectric structure: (a) Structural parameters and incident plane wave; (b) Equivalent network; (c) Simplified equivalent network.

For this kind of plane structure, we can consider respectively the TE wave and the TM wave. The entire electromagnetic field is an overlay of these two kinds of polarized waves. We select a coordinate system so that the incident plane wave does not vary along the *y* axis, that is, the incident surface is the *xz* plane. With this kind of coordinate system, we can express the electromagnetic field in any layer ϵ_i as follows:

For TE waves:

$$E_y^{(i)}(x,z)=V_i(z)e^{-jk_x x} \quad (1)$$

$$H_x^{(i)}(x,z)=-I_i(z)e^{-jk_x x} \quad (2)$$

$$H_z^{(i)}(x,z)=\frac{k_x}{\omega\mu_0}V_i(z)e^{-jk_x x} \quad (3)$$

For TM waves:

$$H_y^{(i)}(x,z)=I_i(z)e^{-jk_x x} \quad (4)$$

$$E_x^{(i)}(x,z)=V_i(z)e^{-jk_x x} \quad (5)$$

$$E_z^{(i)}(x,z)=\frac{-k_x}{\omega\epsilon_0\epsilon_i}I_i(z)e^{-jk_x x} \quad (6)$$

In the above formulas, $k_x=k_0\epsilon_r^{1/2}\sin\theta$ is the x component of the incident wave wave number, that is, the transmission constant of the guide wave, the common quantity for each layer. $V_i(z)$ and $I_i(Z)$ are two functions to be set; their variation pattern can be found by substituting the above two sets of field quantities in the Maxwell equation set. By means of deduction, we obtain the ith layer's transverse (z axis) transmission line equation:

$$\frac{d}{dz}V_i(z)=-jK_iZ_iI_i(z) \quad (7)$$

$$\frac{d}{dz}I_i(z)=-jK_iY_iV_i(z) \quad (8)$$

In the formulas:

$$K_i=(k_0^2\epsilon_i-k_x^2)^{1/2} \quad (9)$$

TE wave
TM wave

$$Z_i=\frac{1}{Y_i}=\begin{cases}\omega\mu_0/K_i & \text{TE波}\\ K_i/\omega\epsilon_0\epsilon_i & \text{TM波}\end{cases} \quad (10)$$

Hereby the two-dimensional electromagnetic field problem is simplified to a one-dimensional transmission line problem. $V_i(Z)$ and $I_i(z)$ are called respectively the (transverse) transmission line voltage and the current; K_i is called the (transverse) transmission constant, and Z_i and Y_i are respectively called the special impedance and the special admittance. The above transmission line equations are suitable for the material of any given layer; the difference is only in the transmission line parameters K_i and Z_i; these are determined by the ϵ_i of the layer and the properties k_0 and k_x of the incident wave.

The original electromagnetic field problem's boundary condition is that at the location ($z = z_i$) of the boundary surface between layer and layer the

actual directional components of the electromagnetic field must be continuous. For the TE wave we have:

$$E_y^{(i)}(x,z_i)=E_y^{(i+1)}(x,z_i) \tag{11}$$

$$H_x^{(i)}(x,z_i)=H_x^{(i+1)}(x,z_i) \tag{12}$$

And for the TM wave we have:

$$H_y^{(i)}(x,z_i)=H_y^{(i+1)}(x,z_i) \tag{13}$$

$$E_x^{(i)}(x,z_i)=E_x^{(i+1)}(x,z_i) \tag{14}$$

Substituting (1)/(2) and (4)/(5) respectively into (11)/(12) and (13)/(14), we obtain:

$$V_i(z_i)=V_{i+1}(z_i) \tag{15}$$

$$I_i(z_i)=I_{i+1}(z_i) \tag{16}$$

It can be seen that the boundary condition for the field problem has changed into a connection condition for a transmission line problem. At the connecting location of the two transmission lines, the voltage and the current are both continuous. We thus obtain the (transverse) equivalent network of our multilayer structure, as shown in Fig. 2(b).

Based on the transmission line theory, if the ith transmission line section encounters a load $Z_{out}^{(i)}$, its input impedance is:

$$Z_{in}^{(i)}=Z_i\,\frac{Z_{out}^{(i)}+jZ_i\tan K_i t_i}{Z_i+jZ_{out}^{(i)}\tan K_i t_i}=Z_{out}^{(i-1)} \tag{17}$$

Repeatedly adducing the impedance transformation formula (17) in an upward direction, we finally obtain the input impedance Z_{in} at the location of the layer separation between the ϵ_p and ϵ_s layers, looking downward. We hereby obtain the simplified equivalent network, as Fig. 2(c) shows.

A. Transmission Characteristics

It can be seen from Fig. 2(c) that the reflection coefficient of the ϵ_p- ϵ_s boundary surface is:

$$\Gamma=\frac{Z_{in}-Z_p}{Z_{in}+Z_p}=\frac{b}{a} \tag{18}$$

The x direction guide wave should be a standing wave in the transverse (z) direction; that is, it should be located in a transverse resonance condition. At this time, if there is no a there still may be a b; therefore the transverse resonance condition is:

$$Z_{in}+Z_{in}=0 \qquad (19)$$

Note that the left side of (19) is a function of k_x; by means of (17), (9) and (10) it is possible to obtain this kind of function relation:

$$f(k_x)=0 \qquad (20)$$

The method of using (19) or (20) to solve for the structure's eigenvalue (transmission characteristics) is called the transverse resonance technique (TRT). Normally, the transmission characteristics are illustrated using a chromatic dispersion graph; substituting $k_x=\epsilon_{eff}^{1/2}k_0$ into (20) gives us the needed chromatic dispersion equation:

$$f_1(\epsilon_{eff})=0 \qquad (21)$$

Examples of using a computer to solve (21), that is, to obtain the chromatic dispersion graph for all kinds of structures, are provided in Section 3 below.

B. Plasma TM Pattern

At this point we shall describe briefly the principle of the plasma surface wave. We know that at microwave frequencies, surface waves do not exist in the boundary surface between the metal conductor and the dielectric (see Fig. 3[a]). Nevertheless, under optical frequencies, the situation is completely different; as we said above, the metal conductor under optical frequencies has a negative value ϵ_m (m = metal). Based on the equivalent network of Fig. 3(b), the resonance condition is:

That is

$$Z_{in}+Z_{in}=0$$

$$Z_{in}+Z_{in}=0 \qquad (22)$$

If a surface wave exists, it is necessary to make:

$$K_{x}=-j|K_{x}| \qquad (23)$$

$$K_{z}=-j|K_{z}| \qquad (24)$$

Using (10), (23) and (24), we can obtain from (22), for a TE wave:

$$|K_3| + |K_m| = 0 \tag{25}$$

and for a TM wave (using $k_x = \epsilon_{//}^{1/2} k_0$):

$$\epsilon_{//} = \frac{\epsilon_m \epsilon_3}{\epsilon_m + \epsilon_3} \quad (|\epsilon_m| > \epsilon_3) \tag{26}$$

(25) has no non-zero solution, so it can be seen in advance that there cannot exist any TE pattern surface wave on the boundary surface. (26) has a zero solution, showing that on the boundary surface there exists a kind of TM pattern surface wave. We call this a plasma surface wave, to distinguish it from the ordinary dielectric boundary surface surface wave. (26) also provides a simple and clear formula for calculating the equivalent dielectric constant of the plasma surface wave, or the relative emission velocity.

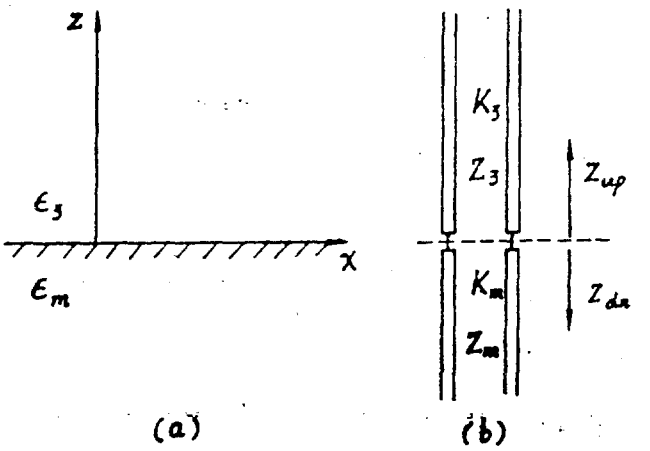

Fig. 3. Boundary surface between plasma and dielectric and its equivalent network.

C. Reflection Characteristics

By means of (18), (17), (9) and (10), it is possible in the same way to find a formula expressing Γ as a function of k_z:

$$\Gamma = \Gamma(k_z) \tag{27}$$

However, $k_z = k_p \sin\theta = \epsilon_p^{1/2} k_0 \sin\theta$; therefore

$$\Gamma = \Gamma(\theta) = |\Gamma(\theta)| e^{j\varphi(\theta)} \tag{28}$$

That is, under conditions of the other parameters being fixed, the reflection coefficient's pattern $|\Gamma|$ and the phase angle ϕ are both coefficients of the angle of incidence θ. Currently, we are only interested in $|\Gamma|$; therefore we emphasize $|\Gamma(\theta)|$. Using a computer to solve formula (28), it is possible to obtain the structure's reflection characteristics (see Section 3 below).

D. Control of the Absorption Angle's Migration

If we cause variation in a given layer's dielectric constant ϵ_1, the reflection coefficient $|\Gamma(\theta)|$ should be the binary function of θ and ϵ_1. Using ϵ_1 as the parameter controlling $|\Gamma(\theta)|$, it is possible to control the variations of $|\Gamma(\theta)|$, that is, to control the absorption angle's migration. In this kind of control pattern, the use of manual calculation is extremely complex and difficult; but using a computer model experiment makes it quite simple; several results are provided in Section 3.

3. COMPUTER MODEL EXPERIMENTAL RESULTS

A. Transmission Characteristics

Figure 4 shows three kinds of chromatic dispersion characteristics for dielectric layer structures. The base of the structure is dielectric ϵ_s, and the upper layer is air ϵ_a. It can be seen from the figure that the TE pattern and the TM pattern appear separated, and do not intersect. For this reason it is not possible to find a common relative speed or a common coupling angle (an angle of incidence phase matched with the plane electromagnetic wave). The cutoff phenomenon of the dielectric wave guide ($\epsilon_{eff}<\epsilon_s$) has a physical substance different from the metal tube wave guide; it does not show that the electromagnetic wave is unable to be transmitted forward, and to be reflected backward, but is radiated from the lower boundary surface in a wave leakage style. When $t_f=0.5\lambda$, the TE pattern and TM pattern are both transmitted in a single pattern.

Calculation shows that the chromatic dispersion curves of dielectric structures with even more layers also have the TE and TM patterns appearing at a remove from each other and not crossing over. Calculation also shows that the small value virtual portion of the dielectric constant (by means of the microscale wear factor) has very little effect on the chromatic dispersion characteristics.

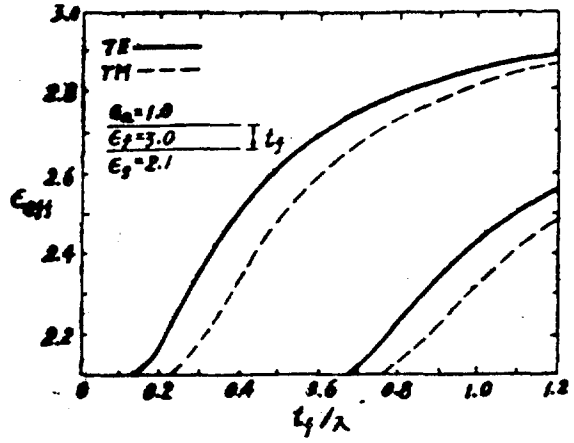

Fig. 4. The chromatic dispersion characteristics of three kinds of dielectric structures.

B. Plasma Surface Waves

Fig. 5 shows, on the basis of the structure in Fig. 4, that if a metal substrate (plasma) is added below, in the same way, when t_f=0.5λ or less, the TM patterns increase by one. In the chromatic dispersion graph, when $t_s \to 0$, the upper TM pattern clearly is a plasma surface pattern because the common surface pattern's ϵ_{eff} may not be larger than ϵ_f, no matter what the value of t_s. But when $t_s \to \infty$, the lower TM pattern is a plasma surface pattern, because, in accordance with (26), at this time its $\epsilon_{eff} \approx 2.41$. When t_s=the limiting value, it is not possible to call them pure plasma surface patterns or common surface patterns; it is only possible to say that the two TM patterns are the

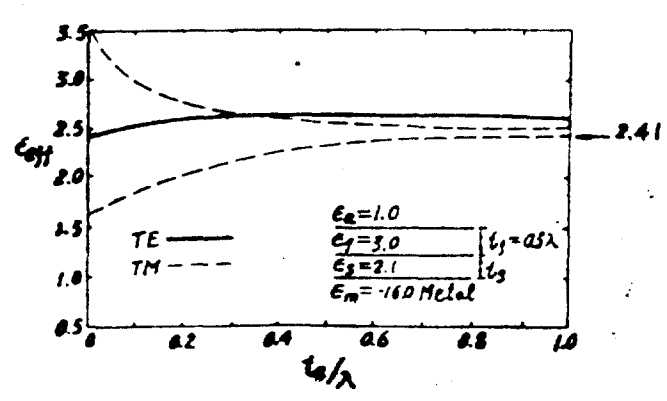

Fig. 5. The chromatic dispersion characteristics for three kinds of dielectric layer structure having a plasma substrate.

structure's eigen patterns (TM_1 and TM_2). It can be seen from Fig. 5 that the graphs of the TE pattern and the TM patterns can cross; this has the effect that below the same angle of incidence simultaneous coupling of the TE wave and the TM wave becomes possible.

C. Reflection Characteristics, Absorption Angle Control, and Automatic Switches

Figure 6 and 7 show how the reflection coefficient of two kinds of multiple layer structures v s in relationship with the third layer's

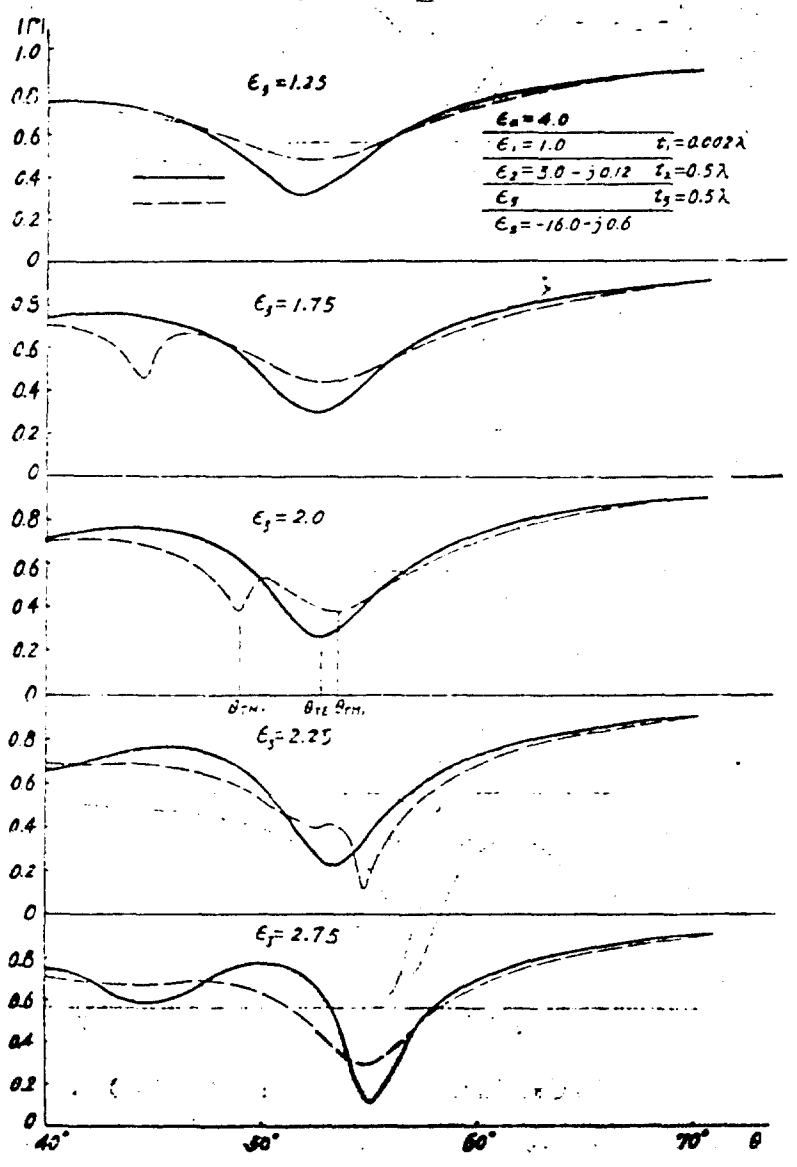

Fig. 6. Shifts in absorption angle owing to changes in ϵ_3 (t_1=0.002 λ).

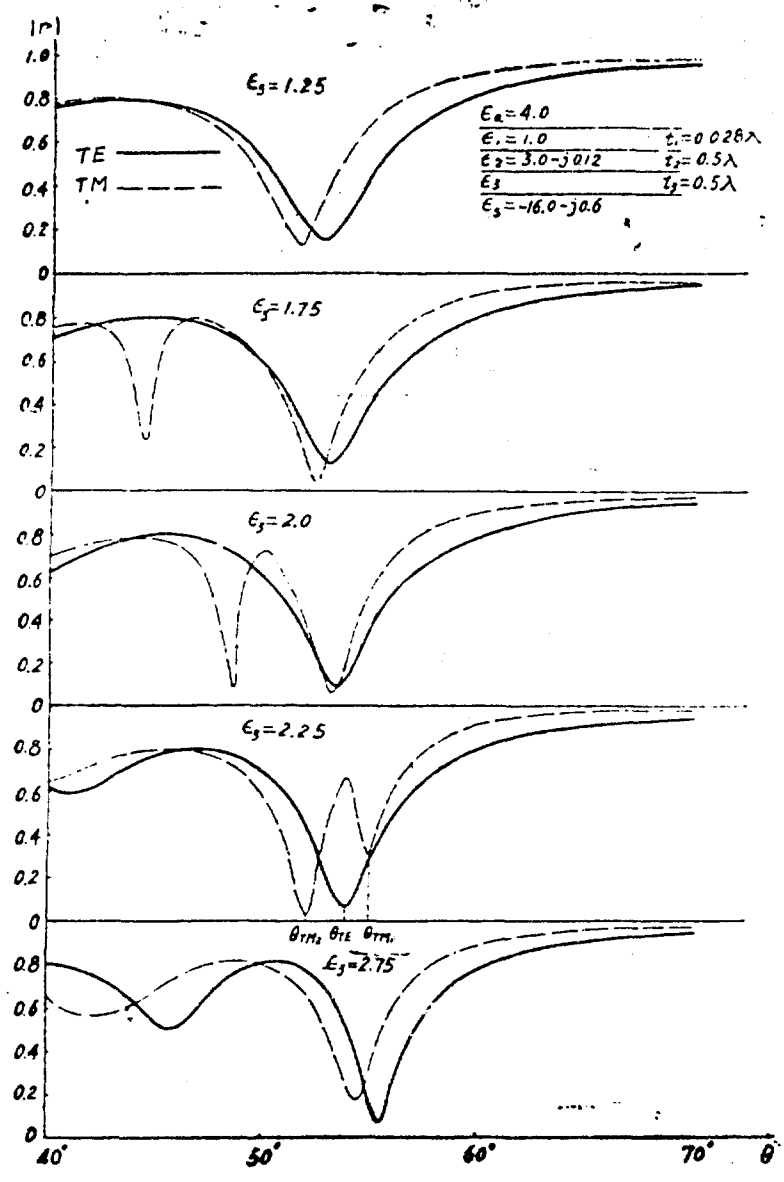

Fig. 7. Shifts in absorption angle owing to changes in ϵ_3 (t_1=0.028λ).

dielectric constant ϵ_3; the difference between the two structures is only the size of the air space t_1; for the former, t_1=0.002 λ, while for the later t_1=0.028λ. From these two figures it is possible to see the following facts: 1) The absorption angles for all patterns, regardless of whether they are TE, TM_1 or TM_2, all increase with an increase in ϵ_3; 2) With identical increases in ϵ_3, there are differences in the size of the shift of all patterns' absorption angle; the shift is fastest for the TM_2 pattern, and

slowest for the TE pattern.

On the basis of the results shown in Fig. 6 and 7, by means of adjustments to ϵ_2'', ϵ_m'' and t_1, it is possible to calculate all kinds of automatic self-protection switches. Based on Fig. 6, we calculated two kinds of switches; the reflection coefficients for these "Number 1" and "Number 2" switches are shown in Fig. 8 and 9. For the sake of comparison, Table 1 shows their parameters and properties.

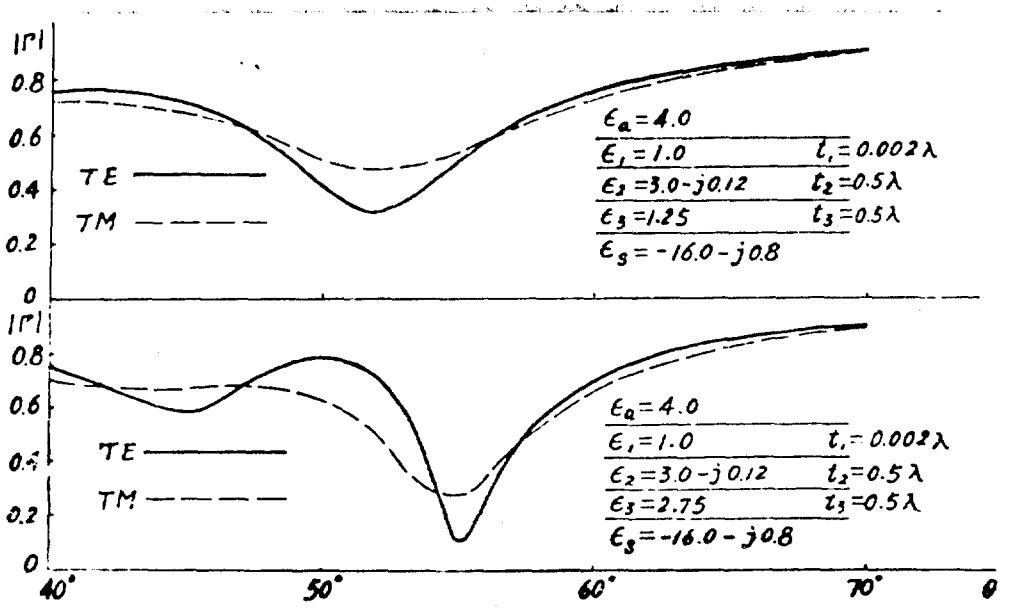

Fig. 8. Reflection coefficient of Number 1 switch.

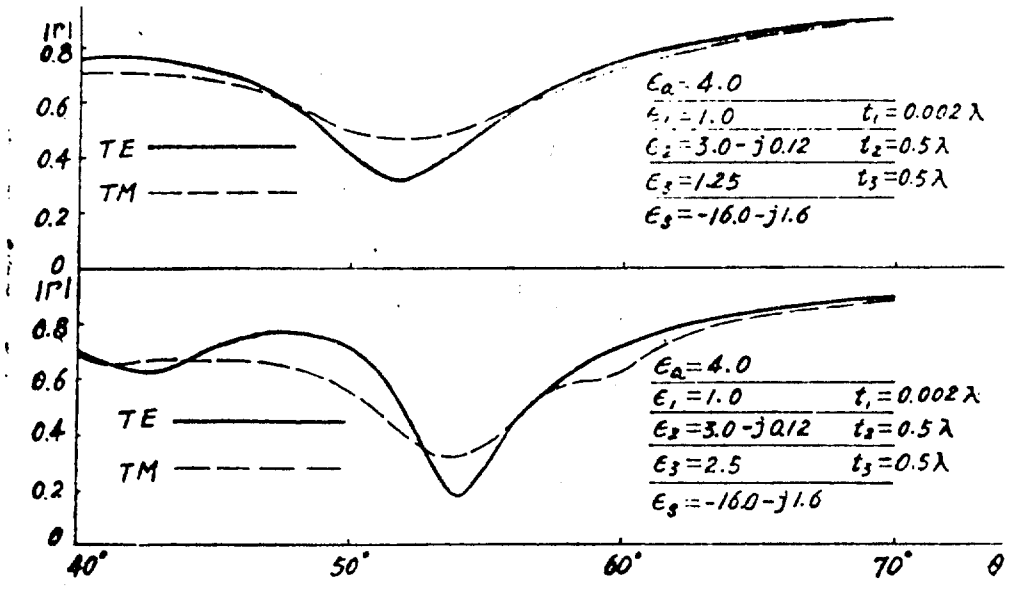

Fig. 9. Reflection coefficient of Number 2 switch.

Table 1. Parameters and properties of Number 1 and Number 2 switches.

(1) 参数和性能 \ (2) 号数	1号 (3)	2号 (4)
t_1	0.002λ	0.002λ
ϵ''_2	0.12	0.12
ϵ''_S	0.8	0.8
$\triangle\epsilon_s$	1.5(1.25→2.75)	1.25(1.25→2.5)
(5) 角移$\triangle\theta$	≈3°	≈2°
(6) 功率比（平均）	≈$\frac{1}{5}$	≈$\frac{1}{8}$

Key to Table 1. (1) Parameters and properties; (2) Number; (3) Number 1; (4) Number 2; (5) Angular shift $\Delta\theta$; (6) Power ratio (mean).

On the basis of Fig. 7, we calculated an additional two switches, Number 3 and Number 4. Their reflection coefficients are shown in Figures 10 and 11, and their parameters and properties are shown in table 2.

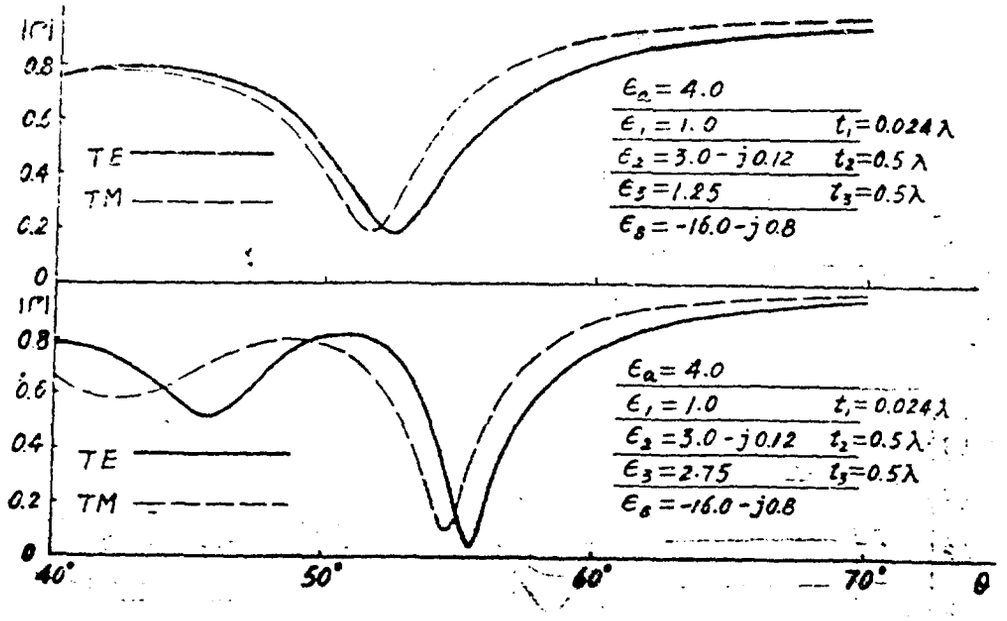

Fig. 10. Reflection coefficient of Number 3 switch.

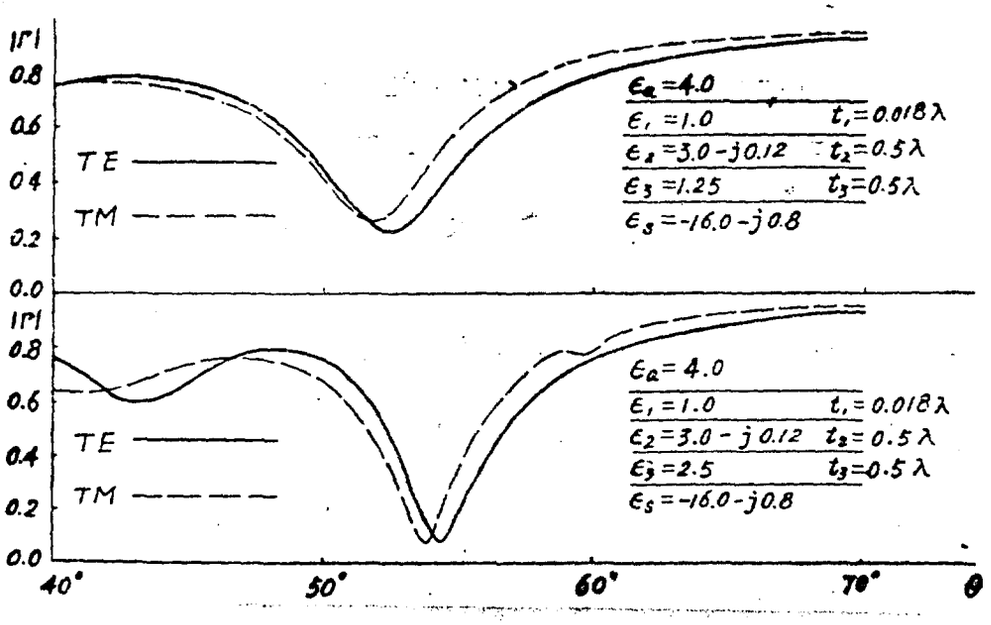

Fig. 11. Reflection coefficient of Number 4 switch.

Table 2. Parameters and properties of Number 3 and Number 4 switches.

(1) 参数与性能 \ (2) 号数	3号 (3)	4号 (4)
t_1	0.024λ	0.018λ
ϵ''_2	0.12	0.12
ϵ''_s	0.8	0.8
$\Delta\epsilon_3$	1.5(1.25→2.75)	1.25(1.25→2.5)
(5) 角移$\Delta\theta$	$\approx 3°$	$\approx 2°$
(6) 功率比（平均）	$\approx\frac{1}{10}$	$\approx\frac{1}{10}$

Key to Table 1. (1) Parameters and properties; (2) Number; (3) Number 3; (4) Number 4; (5) Angular shift $\Delta\theta$; (6) Power ratio (mean).

4. CONCLUSIONS

Theoretical study has shown that the use of a metal substrate is able to cause multilayer dielectric structures to add a plasma TM pattern, and to effect a crossing in the chromatic dispersion graph of the TM pattern and the TE pattern, thereby solving the problems of simultaneous crossing and TE wave and TM wave absorption. If one layer is a non-linear material, variations in the incident light intensity are able to cause migration in the absorption angle of all patterns; in addition, taking advantage of the fact that an "exact" plasma TM pattern absorption angle's migration is very rapid, and using the approach of TM pattern jump/pattern absorption, it is possible to discover automatic self-protecting switches in which the TE and TM wave absorption angles are able to coincide under conditions of strong and weak light.

During this project we have had beneficial discussions with Dr. M.J. Shiau of the New York Institute of Science and Engineering; we wish to express our gratitude at this time.

BIBLIOGRAPHY

1. Li, B.H., M.J. Shiau and S.T. Peng. "Strong Absorption of Light by Multilayer Dielectric-Metal Structures," SPIE Conference, VA, April 1983.

2. Peng, S.T. and A.A. Oliner. "Guidance and Leakage Properties of a Class of Open Dielectric Waveguides: Part I - Mathematical Formulations," IEEE Trans. Microwave Theory Tech., Vol. MTT-29, pp. 843-854, Sept. 1981.

3. Oliner, A.A., S.T. Peng, T.I Hsu and A. Sanchez. "Guidance and leakage Properties of a Class of Open Dielectric Waveguides: Part II - New Physical Effects," IEEE Trans. Microwave Theory Tech., Vol. MTT-29, pp. 855-869, Sept. 1981.

DISTRIBUTION LIST

DISTRIBUTION DIRECT TO RECIPIENT

ORGANIZATION	MICROFICHE
C509 BALLISTIC RES LAB	1
C510 R&T LABS/AVEADCOM	1
C513 ARRADCOM	1
C535 AVRADCOM/TSARCOM	1
C539 TRASANA	1
Q591 FSTC	4
Q619 MSIC REDSTONE	1
Q008 NTIC	1
E053 HQ USAF/INET	1
E404 AEDC/DOF	1
E408 AFWL	1
E410 AD/IND	1
F429 SD/IND	1
P005 DOE/ISA/DDI	1
P050 CIA/OCR/ADD/SD	2
AFIT/LDE	1
NOIC/OIC-9	1
CCV	1
MIA/PHS	1
LLYL/CODE L-309	1
NASA/NST-44	1
NSA/T513/TDL	2
ASD/FTD/TTIA	1
FSL	1